P6.5

AIR TEMPERATURE MEASUREMENT ERRORS IN A NATURALLY VENTILATED MULTI-PLATE RADIATION SHIELD

Reina Nakamura* and L. Mahrt
Oregon State University, Corvallis, OR, USA

1. INTRODUCTION

In observational networks of air temperature, mechanically aspirated radiation shields are often replaced by naturally ventilated radiation shields because of the operational costs and power requirements. The radiative errors need to be assessed for correctly interpreting air temperature data collected in a naturally ventilated shield. If sensor-shield systems within a network of air temperature measurements experience different radiative forcing, e.g. due to variable cloudiness or exposure differences, the horizontal temperature gradient may be incorrectly estimated. In addition, when air temperature measurements are used to evaluate the sensible heat flux from the surface with the bulk-transfer method, the radiative error could cause significant errors in the predicted sensible heat flux and even the wrong sign (Anderson and Baumgartner, 1998).

The HOBO Pro Data Logger (Model H08-031-08, Manufacturer: Onset Computer Corporation) and its external thermistor enclosed in a naturally ventilated multi-plate radiation shield has become one of the commonly used practical systems for long-term air temperature monitoring (Whiteman et al., 2000). A series of field experiments are conducted to investigate the sources and magnitude of the radiative errors of the sensor-shield system. An empirical model is developed for correcting temperature errors using information on wind speed and net or solar radiation.

2. DATA

Data were collected above a flat grassland near Corvallis, Oregon in the spring and summer of 2002 and in the summer of 2003. Air temperature was measured by 1) a HOBO thermistor in the multi-plate shield of Davis Instruments Model 7714 (Figure 1) and 2) a RTD sensor (RM Young, Model 43347) in a mechanically aspirated shield (RM Young, Model 43408) at 1*m* above the ground surface. The accuracies of the HOBO thermistor and the RTD sensor are ± 0.2°*C* and ± 0.1°*C*, respectively. In addition, wind speed, direction and 4 components of radiation were measured.

Figure 1: Naturally-ventilated multi-plate radiation shield (Davis Instruments, Model 7714, dimension: 152 *mm*× 213 *mm*× 188 *mm*). HOBO data logger is attached to the bottom of the shield.

For investigating the sources of the radiative error, shortwave radiation inside the shield was measured with pyranometers. In addition, an infrared transducer was deployed directly above and underneath a multi-plate shield for monitoring the shield surface temperature. A Type-E thermocouple was simultaneously deployed on the top plate of a multi-plate shield.

All the data except for the HOBO thermistor measurements were logged at 0.5 *Hz* by a Campbell Scientific CR23X data logger in 2002 and a CR5000 data logger in 2003. The HOBO thermistor data were logged every 5 *min*.

3. SOURCES OF RADIATIVE ERROR

The ray tracing study of Richardson et al. (1999) showed that solar radiation entering a multi-plate shield is mostly absorbed by the shield or sensor, contributing

*corresponding author address: Reina Nakamura, College of Oceanic and Atmospheric Sciences, Oregon State University, Corvallis, OR; email: reina@coas.oregonstate.edu

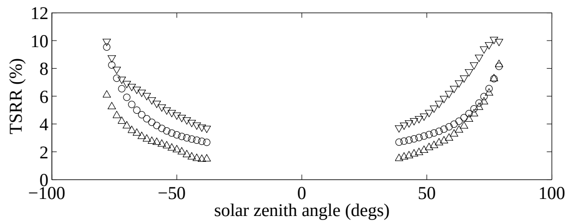

Figure 2: *TSRR*% for grass-covered (◦), black (△) and white (▽) ground surfaces. A negative (positive) sign in the solar zenith angle indicates before (after) solar noon. Because of limited space within the shield, downward and upward radiation were measured separately, on two different cloudless days.

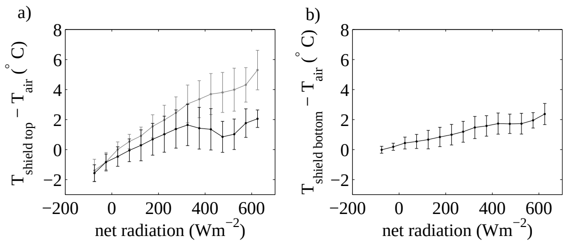

Figure 3: Bin-averaged deviation of the shield surface temperature from air temperature (aspirated) as a function net radiation above the grass surface: a) shield top, b) shield bottom. The shield top temperature was simultaneously monitored by a thermocouple (gray) and an infrared transducer (black). Vertical bars indicate standard deviations within bins.

to the radiative error. The degree of shortwave radiation reaching inside a radiation shield may be represented as the total shortwave radiation ratio, *TSRR*% (Hubbard et al., 2001), defined as

$$TSRR\% = 0.5(DSRR\% + USRR\%) \tag{1}$$

where *DSRR*%and *USRR*% are downward and upward shortwave radiation ratios, respectively, defined as

$$DSRR\% = \frac{Downward\ solar\ irradiance\ inside\ shield}{Incoming\ global\ solar\ irradiance} \times 100 \tag{2}$$

and

$$USRR\% = \frac{Upward\ solar\ irradiance\ inside\ shield}{Incoming\ global\ solar\ irradiance} \times 100 \tag{3}$$

Downward (upward) shortwave radiation measurements were made by an upward (downward) facing pyranometer situated at 2.5*cm* (3.5*cm*) height in the inner space of the shield, where the HOBO thermistor is typically placed. To investigate the influence of shortwave radiation reflected from the ground surface, the pyranometers enclosed in the multi-plate shields were deployed over three surface types: the original grass (albedo: 0.23), a black surface (albedo: 0.08) and a white surface (albedo: 0.56). The size of the black and white surfaces was $6m \times 6m$.

Both *DSRR*% and *USRR*% reach maximum values at high solar zenith angles (Figure 2) although the absolute magnitude of the shortwave radiation detected inside the shield at such zenith angles is at a minimum. Shortwave radiation reaching inside the shield is positively correlated with surface albedo, which implies a significant portion of the shortwave radiation reaching inside the shield originates from shortwave radiation reflected from the ground surface. Thus, the radiative error due to the direct solar heating of the sensor inside the present multi-plate shield likely increases with increasing surface albedo.

Deviation of the shield temperature from the air temperature is another source of radiative error. It modifies the air temperature inside the shield by sensible heat transfer and at the same time, modifies the sensor temperature by longwave radiative transfer. The relevant deviation of the shield temperature here is that of the inner surface of the shield. With existing instrumentation, we were able to measure only the outside shield temperature. We assume that the conductivity of the shield material is sufficiently high that changes of the inner and outer surface temperatures of a given plate are highly correlated.

The shield-top temperature measured by the thermocouple and that by the IR transducer agree at night (Figure 3). However, the thermocouple estimates of the shield-top warming are systematically larger than the IR transducer during daytime probably because of the combination of self-shadowing of the IR transducer at low solar zenith angles and solar heating of the thermocouple wires. The actual shield-top daytime temperature is tentatively considered to be somewhere between the two estimates. The systematic positive and negative deviation of the multi-plate shield surface from the ambient air temperature occurs for daytime and nighttime, respectively, which could contribute to the radiative error.

The above sources of radiative error are counteracted by increasing the degree of coupling of the air inside the shield to the ambient air. Unfortunately, increasing coupling requires wider separation distance between the shield plates and therefore more direct shortwave radiation enters the shield interior.

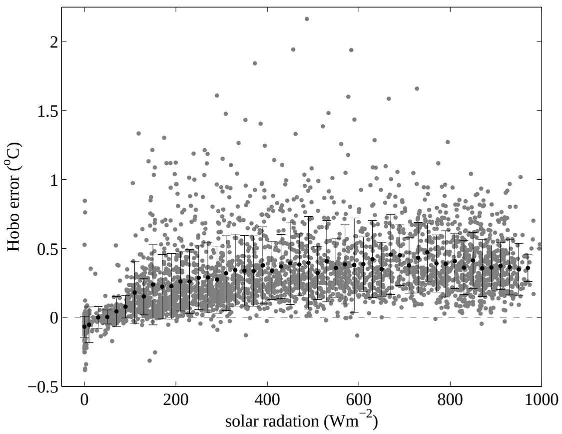

Figure 4: The original (gray circles) and bin-average values (black circles) of the HOBO radiative errors for all the 2002 data. The error bars indicate the standard deviations. The bin width is 20 Wm^{-2} except all the HOBO radiative errors in shortwave radiation of 0 Wm^{-2} (nighttime) are averaged all together.

4. HOBO RADIATIVE ERROR

Rigorous correction of radiative errors may require radiation and air flow measurements inside the shield which are not necessarily linearly correlated with those outside the shield. However, radiation and air flow measurements inside the shield are not readily available. We attempt to pragmatically correct for the radiative error using only information on wind speed, shortwave and longwave radiation measurements made outside the shield.

With the data collected in 2002, the HOBO radiative error is estimated as the deviation of 30-min mean temperature estimated by the HOBO thermistor from that estimated by the RTD sensor. We assume that the radiative error for the RTD sensor in the mechanically aspirated shield is small. The manufacturer′s specification states that shortwave radiation measurements are unreliable when solar elevation is less than 10°. Thus, such data are discarded. The wind speed data are scalar- rather than vector-averaged over 30 *min* because instantaneous wind speed, regardless of the wind direction, ventilates the thermistor-shield system.

A day can be classified into three periods: daytime, nighttime and transition periods (Figure 4). During the daytime when shortwave radiation is larger than 20 Wm^{-2}, the HOBO radiative error becomes systematically positive. At nighttime, when the net radiation is negative, the HOBO radiative error becomes negative. The transition period is defined as the period when the shortwave radiation is larger than 0 Wm^{-2} and less than 20 Wm^{-2}. In this period, the radiative error is weakly negative although the solar radiation is positive; the net radiation can take either positive or negative value. In the transition period, highly non-stationary atmospheric conditions make the prediction of the radiative error complex. Thus, we attempt to correct the radiative errors only in the daytime and nighttime periods.

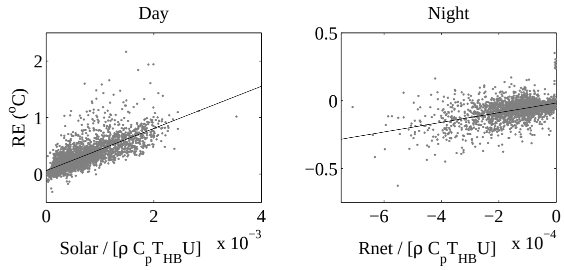

Figure 5: HOBO radiative error as a function of scaled radiation forcing X. Lines indicate regression lines based on the determined coefficients (daytime: $C_1 = 0.06$, $C_2 = 373.30$; nighttime: $C_1 = -0.02$, $C_2 = 355.82$)

We propose expressing the radiative error in terms of the ratio of the radiative forcing to the ambient wind speed represented by the non-dimensional number X:

$$X = \frac{Rad}{\rho C_p T_{HB} U} \tag{4}$$

where Rad $[Wm^{-2}]$: shortwave radiation and net radiation for the daytime and nighttime, respectively, U $[ms^{-1}]$: wind speed, ρ $[kgm^{-3}]$: density of air, taken to be 1.2, C_p $[JK^{-1}kg^{-1}]$: specific heat capacity of air at constant pressure, T_{HB} $[K]$: HOBO temperature.

The relationship between the radiative error, RE and non-dimensional number X is formulated as a polynomial regression relationship

$$RE = C_1 + C_2X + C_3X^2 ... \tag{5}$$

where C_1, C_2 and C_3 are empirical coefficients that presumably depend on characteristics of the thermistor-shield system and those environmental flow characteristics not included in X.

The radiative error correction is most needed when the wind speed is low and radiative forcing is high (Section 3), that is when X is large. However, such conditions occurred less frequently than conditions with significant wind or cloudiness which induce small radiative error. For determining the coefficients in the model in Equation (5), the original 30-min data of the HOBO error are averaged for intervals of the non-dimensional number, X, equal to 1.25×10^{-4} and 2.5×10^{-5} for daytime and

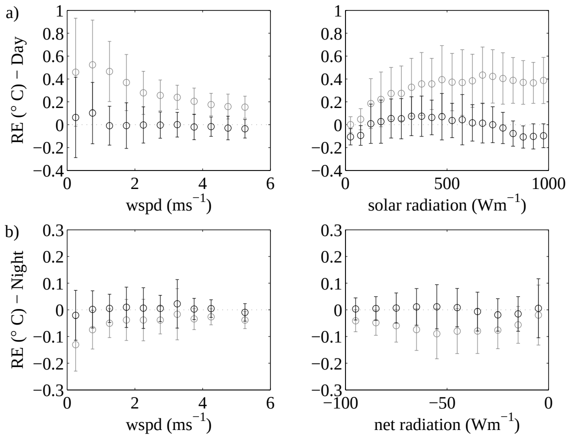

Figure 6: Statistics of bin-averaged HOBO radiative errors for 30-min mean air temperature as a function of wind speed (left) and shortwave or net radiation (right): a) day, b) night periods. Gray and black HOBO errors indicate those before and after corrections (Equation (5)), respectively. The vertical bars indicate the standard deviation within each bin.

nighttime, respectively. Equation (5) is regressed on the bin-averaged data to determine the coefficients.

The hindcast skill of a model always improves by adding more parameters. Therefore, the statistical significance of the increased hindcast skill is examined with the analysis of variance as in Chelton (1983) after an each higher order term is added to the model (Equation 5). The hypothesis that the additional parameter did not improve the true regression model is tested with 95 percent confidence level by assuming that the individual bin-averaged data are assumed to be statistically independent. The results indicate that adding higher orders beyond the first order term does not improve the regression model. Figure 5 shows the fit of the determined model to the original data (daytime: $C_1 = 0.06$, $C_2 = 373.30$; nighttime: $C_1 = -0.02, C_2 = 355.82$).

The use of the error prediction model with the determined coefficients reduces the radiative error substantially, especially in calm and sunny daytime conditions (Figure 6). The mean and the root mean square error are significantly reduced in both daytime and nighttime (Table 1). The present model does not include all the physical processes affecting the radiative error, which partly accounts for the residual of the model-predicted radiative error. For example, characteristics of air flow such as steadiness and turbulent intensity, on which air flow rate within a multi-plate shield depends, are not included in the model. As an additional example, change in the cloud-cover within the averaging time is not considered.

Finally, the robustness of the error prediction model is examined with the data collected at the same site, but in the summer of 2003 (Section 2). The radiative error is also reduced for the 2003 data effectively (Table 1).

Table 1. Statistics of original and corrected HOBO radiative error for 2002 and 2003 data. RMSE stands for root mean square error. Units: $(°C)$

		2002		2003	
		Mean	RMSE	Mean	RMSE
Day	original	0.32	0.32	0.23	0.23
	corrected	0.004	0.11	-0.08	0.14
Night	original	-0.07	0.08	-0.09	0.10
	corrected	0.0005	0.05	-0.02	0.04

5. ACKNOWLEDGMENTS

The present work is supported by NASA Earth System Science Fellowship ESS/01-0000-0116 and NASA Terrestrial and Ecology Program Grant NAGS5 11231.

REFERENCES

Anderson, S.P. and M.F. Baumgartner, 1998: Radiative heating errors in naturally ventilated air temperature measurements made from buoys. *J. Atm. Oc. Tech.*, **15**, 157-173.

Chelton, D.B., 1983: Effects of sampling errors in statistical estimation. *Deep-Sea Res.*, **30**, 1083-1103.

Hubbard, K.G., X. Lin, and E.A. Walter-Shea, 2001: The effectiveness of the ASOS, MMTS, Gill and CRS air temperature radiation shields. *J. Atm. Oc. Tech.*, **18**, 851-864.

Richardson, S.J., F.V. Brock, S.R. Semmer and C. Jirak, 1999: Minimizing errors associated with multiplate radiation shields. *J. Atm. Oc. Tech.*, **16**, 1862-1872.

Whiteman, C.D., J.M. Hubbe and W.J. Shaw, 2000: Evaluation of an inexpensive temperature data logger for meteorological applications. *J. Atm. Oc. Tech.*, **17**, 77-81.